

Slow-Mode Induced Pulsing in Trickle-Bed Reactors at Elevated Temperature

Bora Aydin

Dept. of Chemical Engineering, Laval University, Québec, Canada G1K 7P4

Donata Fries

Dept. of Chemical Engineering, Laval University, Québec, Canada G1K 7P4; and Institute of Process Engineering, ETH Zurich, Sonneggstr. 3, 8092 Zurich, Switzerland

Rüdiger Lange

Dept. of Chemical Engineering, Dresden University of Technology, Münchner Platz 3, 01062 Dresden, Saxony, Germany

Faïçal Larachi

Dept. of Chemical Engineering, Laval University, Québec, Canada G1K 7P4

DOI 10.1002/aic.11001

Published online September 25, 2006 in Wiley InterScience (www.interscience.wiley.com).

Periodic operation, as a process intensification measure for trickle beds, is still tepidly greeted by industry despite numerous benefits underlined in the literature. This state of aloofness is partly ascribed to the paucity of experimental data acquired under elevated temperature and pressure, which, in practice, most catalytic reactions are subjected to. Currently, the hydrodynamics of trickle bed periodic operation at elevated temperature and pressure remains by and large an uncharted territory. This study specifically approaches from a hydrodynamic perspective the pros and cons of slow-mode induced pulsing for Newtonian and non-Newtonian power-law liquids at elevated temperature and moderate pressure. Four morphological features of the liquid holdup periodic pattern were analyzed: shock wave breakthrough, shock wave decay times, shock wave plateau, and shock wave breakthrough amplitude. The shock wave decay and breakthrough times were found to shorten, while correspondingly the shock wave plateau to lengthen, with increasing pressure and temperature. Conversely, the breakthrough amplitude of the shock wave underwent palpable collapse the higher the temperature (and/or pressure). The collapse of the bursting pulses with increasing temperatures and pressures was the result of the reduction of base and pulse liquid holdup levels, delivery of liquid cargo from pulse to baseline flow, and occurrence of dispersive hydrodynamic effects with a tendency to flatten the pulses. Qualitatively, similar effects of temperature and pressure were equally observed whether Newtonian or non-Newtonian liquids were used. The less sensational contrasts prevailing between base and pulse holdups might question the opportunity for implementing induced pulsing strategies in high-temperature, high-pressure tall trickle beds. © 2006 American Institute of Chemical Engineers AIChE J, 52: 3891–3901, 2006

Keywords: trickle bed, elevated temperature, hydrodynamics, liquid holdup, induced pulsing, non-Newtonian fluids

Introduction

Trickle-bed reactors (TBR) are among the most pervasive configurations industry makes use of, where gas and liquid

streams downwardly traverse a porous randomly-packed catalyst layer. Despite the fact that continuous-flow TBR operation still typifies an overwhelming orthopraxy, a growing literature is advocating the merits of liquid-induced pulsing as a process intensification means for promoting a multitude of facets of TBR performances.^{1–5}

In liquid-induced pulsing flow, a continuous flow of gas encounters a binary-coded liquid stream that is forced to switch

Correspondence concerning this article should be addressed to F. Larachi at faical.larachi@gch.ulaval.ca.

periodically at the bed entrance between a low-level (also referred to as base) and a high-level (or pulse) velocity. Such a procedure is known to mitigate mass-transfer resistances and to enhance reactor conversion, especially for gas-limited reactions.² Controlling, in addition, wetting efficiency as a function of time enables averting catalyst life time loss and certain undesirable secondary reactions, on top of quenching incipient hot spots and curbing flow maldistribution.³

Induction of pulses can be accomplished by switching liquid velocity, back and forth, either between zero and a specified value, that is, so-called “on-off mode,” or between non-zero base and high-level pulse values, that is, so-called “base-pulse cycling.” In terms of characteristic times, such an unsteady operation can be effected in slow mode for liquid feed periodic changes over few-minute time spans, or in fast mode using brief liquid pulse incursions lasting for a few seconds.

The *spontaneous* pulse flow regime takes place at high enough fluid throughputs in TBRs, achieving therein the high transfer rates^{6,7} that can be tentatively taken advantage of by liquid-induced pulsing emulation. For a given bed length, on the other hand, trickle flow regime offers longer residence times than pulse flow regime. Therefore, superimposing high enough pulse velocity, causing pulse flow regime, onto low enough base velocity, retrieving trickle flow, enables liquid-induced pulsing to embody the two antagonistic, yet both desirable, features into one single flow pattern.

The vast majority of experimental work performed to demonstrate the advantages of periodic operation was directed towards probing the changes undergone by the catalytic reaction response. Experimental studies in reaction systems began to appear in the early 1990s. Haure et al.⁸ studied the influence of periodic water flow on SO₂ catalytic oxidation, whereby 30–45% increase in reaction rate was reported. Lange et al.⁹ studied the hydrogenation of α -methylstyrene under periodic liquid operation up to 1 MPa and 40°C and observed up to 10% increase in the time-average α -methylstyrene conversion. Tukac et al.,¹⁰ studying periodic-operation in the temperature range of 125–170°C and pressure range of 1–7 MPa, improved phenol oxidation conversion by about 10% with respect to that measured at steady state. Wilhite et al.¹¹ reported 45% improvement in product selectivity for the catalytic hydrogenation of phenylacetylene into styrene during induced pulsing flow at 90°C and up to 1.5 MPa. More recently, Urseanu et al.¹² examined the effect of periodic operation for the hydrogenation of α -methylstyrene at 40°C and 0.2 MPa, and pinpointed an improvement of 50% in reaction rate.

Apart from investigations on chemical response enhancement, “fluid mechanics” experimentation on induced pulsing flow has been scantier. Xiao et al.,¹³ by binarizing air flow *feed* rate, achieved a better approach to uniformity of axial and radial liquid distributions in forced pulse flow than for spontaneous pulse flow. Forced air feed superficial velocity and pulse frequency were responsible for further fall off of the liquid holdup. Investigations on liquid flow modulation were instigated by Drinkenburg and coworkers for different particle sizes using an electrical conductivity technique to measure shock wave velocity and liquid holdup under liquid-induced pulsing flow. Hence, Boelhouwer et al.¹ distinguished between slow mode and fast mode feed strategies, and measured shock wave characteristics such as shock wave velocity, shock wave tail and plateau, and pulse frequency. The literature reported

that shock waves decay while moving down the column by leaving liquid behind their tail.¹ This effect is conducive to eroding the shock wave plateaus, which are progressively torn off, according to a linear pattern, as a function of bed depth,¹ while, in return, an increase in the duration of the shock wave tail is diagnosed. The shock wave decay rate, expressed as the decrease in shock wave plateau duration per unit distance, was found to correlate well with the shock wave velocity.¹ In cases of too short durations of base liquid feed, the individual shock waves may start to merge with each other at some depth in the bed, thus erasing any positive effect of induced pulsing. Similarly, a decrease in shock wave tail with increased base liquid superficial velocity was observed. Giakoumakis et al.¹⁴ carried out fast mode liquid-induced pulsing flow experiments on the air-water system. Pulse attenuation was reported from cross-sectionally averaged liquid holdup measurements using ring electrical conductivity probes placed along a glass-bead bed. Experimental data on liquid holdup, pressure drop, and pulse velocity were discussed in terms of gas and liquid flow rates and liquid feed frequency. It is noteworthy that as far as experimental studies on induced pulsing flow characteristics are concerned, none of them afforded interrogating the effects of elevated temperature and pressure.

As the vast majority of industrial trickle bed applications obtrude stiff stream operation, increasing temperature and pressure become virtually inescapable. Any prospect of induced pulsing for industrial implementation therefore dictates further fundamental investigations spotting expressly the incidence of temperature and pressure. Because detailed information about shock wave behavior is important for an operation at optimal conditions, it is the intent of our present study to unveil some of the effects of temperature and pressure on the slow-mode induced pulsing characteristics.

Experimental Setup

The experiments were performed using a stainless steel 48 mm I.D. and 1070 mm long single-module column capable of withstanding temperatures up to 100°C and pressures up to 5 MPa (see Figure 1). Details of the experimental setup were given elsewhere.¹⁵ Nonporous glass beads with a diameter of 3 mm were used as the packing, yielding bed porosity equal to 0.39.

The slow-mode induced pulsing characteristics, in addition to the shock wave velocity and pulse frequency, concerned four morphological features of the dynamic evolution of the liquid holdup: i) the shock-wave breakthrough time, B_{τ} , which measures the transient time for the liquid holdup to rise from base level to pulse value when liquid feed rate is tipped up; ii) the decay time, D_{τ} , which corresponds to the time elapsed for the liquid holdup to retrieve back its base level when liquid pulse feed is tipped out; iii) the shock-wave plateau time, P_{τ} , which measures the duration, intertwined between the breakthrough and decay times, over which *pulse* liquid holdup remains at, or fluctuates around, a constant value; and iv) the shock-wave breakthrough amplitude, B_{α} , which measures the increment of liquid holdup between the base and pulse levels. Figure 2a pictorially sketches each of these four features.

Among the previous quartet, the breakthrough amplitude is the only non-temporal property extracted from the liquid holdup time series. This property is computed as an ensemble-

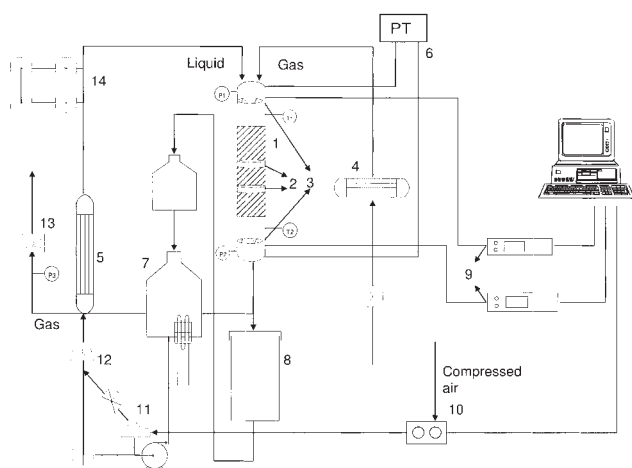


Figure 1. Experimental setup: (1) packed bed, (2) ring electrical conductivity probes, (3) RTD electrical conductivity probes, (4) gas preheater, (5) liquid preheater, (6) pressure transducer, (7) reservoir, (8) gas-liquid separator, (9) lock-in amplifiers, (10) three-way solenoid valve, (11) on-off valve for the additional liquid feed, (12) liquid flowmeter, (13) gas flowmeter, (14) tracer injection loop.

and time-average liquid holdup increment advected by the pulse on top of the base liquid holdup. It is computed after determining the pulse duration, τ_{pulse} , and the number of pulses, N_{pulse} , acquired in each experiment for a given bed depth:

$$B_{\alpha} = \langle \varepsilon_{Lp} - \varepsilon_{Lb} \rangle = \frac{1}{N_{pulse}} \sum_{i=1}^{N_{pulse}} \frac{1}{\tau_{pulse}} \int_0^{\tau_{pulse}} (\varepsilon_{Lp} - \varepsilon_{Lb}) dt \quad (1)$$

The experiments were performed to study the effects of temperature and pressure for Newtonian and non-Newtonian liquids between 25°C and 75°C and up to a pressure of 0.7 MPa. For all the experiments, air was used as the gas phase, whereas water or aqueous 0.25% w/w carboxymethylcellulose (CMC) solution were the process liquids. Note that ease and commodity were the basic criteria that drove our choice of CMC to obtain a model fluid mimicking pseudo-plastic power-law behaviors—besides the obvious industrial relevance of viscous pseudo-plastic fluids in areas such as biotechnology and bio-treating in fixed beds.¹⁶

The CMC solution, prepared by dissolving powdered CMC in water at ambient temperature, exhibited an inelastic pseudoplastic rheological behavior that was well represented by means of a simple power-law Ostwald-DeWaele model. The consistency index, k , and the power-law index, n , were fitted for each process temperature after measuring the solution shear stress-shear rate response on an ARES (Advanced Rheometric Expansion System) rheometer in the 0-1000 s⁻¹ shear-rate ranges. The physical properties of this solution are given in Table 1.

After the liquid was preheated in the reservoir (up to max. 60°C), it was pumped by means of a rotary valve pump through

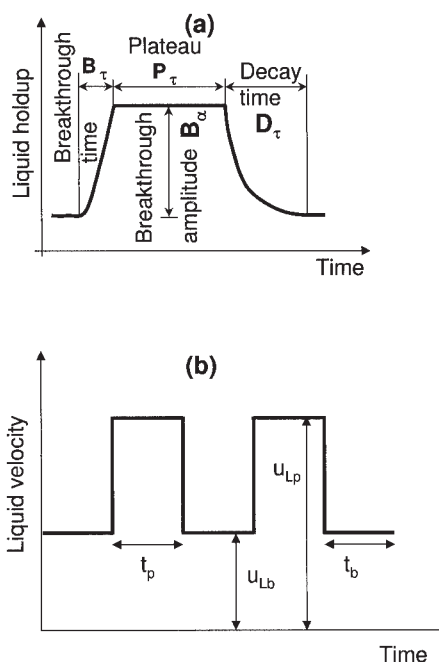


Figure 2. Illustration of the parameters characterizing: (a) morphological features of liquid holdup under cycled liquid feed and (b) square-wave cycled liquid feed.

t_b = base liquid feed period, t_p = pulse liquid feed period, u_{Lb} = base superficial liquid velocity, and u_{Lp} = pulse superficial liquid velocity.

a liquid preheater via calibrated flowmeters, then to the reactor. The line used for feeding the liquid from the pump to the preheater was divided into two streams. The first line was used for handling the continuous liquid flow corresponding to the base (or low-level) feed by means of a controlled valve. The second line was used to supply the additional liquid feed required during the high-level (or pulse) feed. An on-off valve that was actuated by a digital timer was placed on the second line to trigger and shut off the shock wave bursts. With this strategy it was feasible to obtain base (u_{Lb}) and pulse (u_{Lp}) liquid superficial velocities over a wide range of operating conditions. The period for the base and pulse liquid feed was kept to 60 seconds for the air-water system and to 120 seconds for the air-0.25% CMC system. The four common parameters used to characterize the feed square-wave cycled liquid feed are schematically shown in Figure 2b.

The preheaters for the gas and the liquid phases, which were installed before the reactor entrance, were utilized in order to maintain constant target reactor temperatures during the slow-mode induced pulsing experiments. The gas and liquid feeds

Table 1. Physical Properties of Water—0.25% CMC at Elevated Temperatures

Temperature (°C)	k^S (kg/m · s ²⁻ⁿ)	n^S (—)	σ (N/m)
25	0.072	0.67	0.056
50	0.041	0.71	0.054
75	0.033	0.66	0.051

^SConsistency index standard-deviation $\sigma_k = 0.021$.

^SPower-law index standard-deviation $\sigma_n = 0.026$.

were distributed from the top of the column across a distributor designed in a way to achieve homogeneous distribution. After leaving the reactor, the gas-liquid stream was demixed into a separator before cooling down and pressure release. The gas was then released from the separator to the atmosphere via a calibrated flowmeter, while the liquid was recirculated back into the feed tank.

For the measurements of induced pulsing flow characteristics, two electrical conductivity probes of the design adopted by Tsochatzidis and Karabelas¹⁷ and Boelhouwer et al.² and described in more detail elsewhere,¹⁵ were placed in the middle of the reactor with a separation distance of 245 mm. Each probe, consisting of two ring electrodes 1 mm thick and 30 mm apart, was connected to a lock-in amplifier to acquire the output signal. After amplification, the signals were transmitted to a computer by means of a data acquisition system. In order to convert the conductance signals issued from two different axial positions in the bed into liquid holdup ones, the conductivity probes were calibrated by means of two additional residence time distribution (RTD) probes using salt injection and Aris's imperfect impulse method with downstream double detection. At constant temperature, pressure, and superficial gas velocity, the output signals of the two RTD electrical conductivity probes—buried in thin porous medium layers, one at the top and another at the bottom of the column—were received by an electrical conductimeter and transmitted to a computer by a data acquisition system. Liquid residence time distribution curves were obtained by fitting the measured outlet tracer normalized response conductance signal to a two-parameter axial-dispersion impulse response RTD model convoluted to the measured inlet tracer normalized response conductance signal. The space time (τ) was determined by using non-linear least-squares fitting and a time-domain analysis of the non-ideal pulse tracer response data. The thus determined liquid holdup values versus the conductance values received from the two ring probes at the same operating conditions were so plotted to obtain individual calibration curves for each ring probe. This procedure was repeated for different superficial liquid velocities at different constant temperature, pressure, and superficial gas velocity values. Typical calibration curves and relationships between the electrical conductance measured with the ring electrodes and the RTD-determined liquid holdup are shown in Figure 3. The difference between the two calibration lines in Figure 3 presumably arises from the peculiar design discrepancies, which affect the responses of the two pairs of conductance probes. The non-zero intercept, which merely corresponds to progressively drained bed conditions, is irrelevant to our conditions as the bed never comes close to static liquid holdup. This was systematically confirmed from our RTD-calibrated liquid holdups for the flow rate ranges where induced-pulsing was investigated.

In addition, the pulse frequency was determined with an algorithm implemented in MATLAB for counting the number of peaks (holdup maxima or minima) occurring in the conductance signal and dividing by the observational time window locked on the pulse portion or the base (if pulse flow regime is observed there) portion of the liquid holdup time series. On the other hand, the velocity of the shock waves was determined by dividing the distance between the two ring-electrode probes (that is, 245 mm) by the time delay of maximum cross-correlation between signals obtained at pulse superficial liquid ve-

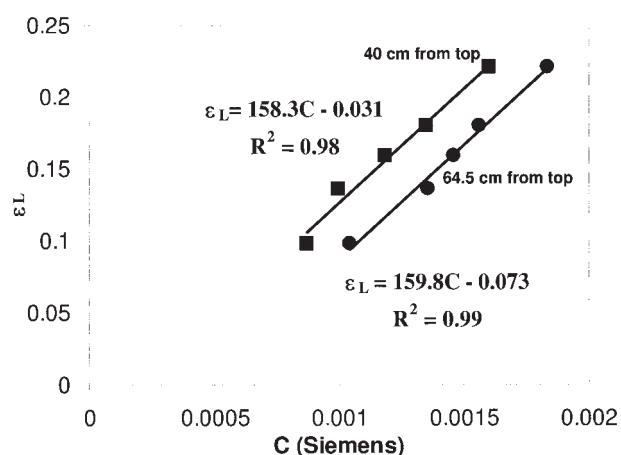


Figure 3. Example of experimental liquid holdup vs. conductance plot for the calibration of the conductance probes for the air-water system.

$T_r = 75^\circ\text{C}$, $P_r = 0.3$ MPa, and $u_G = 0.21$ m/s.

locity. The cross-correlation function will peak at the time delay equal to the time required for the pulses to move from first probe to second probe.

Results and Discussion

Shock wave patterns vs. bed depth

The influence of liquid induced pulsing was studied with respect to the behavior of liquid holdup, ϵ_L , at three temperature and two pressure levels. Regardless of the combination of base and pulse liquid velocities, a constant split ratio of 50% was used for both liquids. Figures 4a and b exemplify typical liquid holdup traces from the two conductivity probes for the air-water and air-0.25% CMC systems, respectively. The runs were conducted at 75°C and 0.7 MPa and at a gas superficial velocity of 0.2 m/s in the slow-mode of operation. The conductivity probes were embedded deep in the bed at 40 cm and 64.5 cm. In terms of systems dynamics, the trickle bed can be viewed as a filter whose impulse response is convoluted with the inlet liquid feed policy to generate signals such as those shown in Figure 4.

During their flight down the bed, the induced pulses undergo alterations with bed depth, which, at first glance, reflect in attenuation in the amplitude of the pulse liquid holdup response. This behavior prevails irrespective of temperature and pressure levels, while similar observations were arrived at by previous investigators for ambient temperature and atmospheric pressure conditions.^{1,14} As water pulses progress downstream (Figure 4a), depletion of the pulse amplitude appears to be quickly taken up by the baseline holdup, which re-equilibrates, within times much shorter than the cycle period, at a higher *compensatory* liquid holdup value. This would indicate that pulses and bases are not hermetically sealed to each other, and that mixing takes place in-between by driving some of the liquid cargo from the pulse down into the baseline flow. Conversely, the 0.25% CMC aqueous solution (Figure 4b), being much more viscous, exhibits less leakage of liquid from the plateau with virtually undisturbed baseline liquid holdup during pulse migration. Presumably because more viscous liquids

drain more slowly, liquid leakage from the plateau reverberates mainly in the long-lasting transient decay branch. Note the larger fluctuations of liquid holdup in the plateau region for the air-0.25% CMC system, which indicate that pulse flow regime had occurred because of the larger liquid holdups attained therein.

From the above observations, it is not difficult to foresee that shock waves may vanish at some bed depth should the TBR be sufficiently tall, a phenomenon already documented for the ambient conditions by Boelhouwer et al.¹ Ultimately, induced pulsing may be supplanted by a *smoothed out* continuous-flow TBR operation that would take over at a constant liquid velocity equal to the weighted average base/pulse velocities. It is instructive, therefore, to assess to what extent such loss in shock wave capacity evolves as temperature and pressure rise beyond ambient conditions.

Shock wave patterns versus temperature

Figures 5a and b show the effect of temperature on the shock waves, respectively, for the air-water and air-0.25% CMC systems at a constant pressure of 0.3 MPa with the ring electrodes buried at a depth of 40 cm. Identical liquid feed policy parameters were used for the different temperatures concerning each liquid. As can be seen from the figures and in line with the trend depicted for the continuous-flow TBR operation,¹⁵ hotter, and thus less viscous, liquids occasion increasingly less liquid holdups. Also, coherent with the corresponding less viscous behavior, increased temperatures appeared to aggravate depletion of the shock wave. Such collapse in pulse amplitude is

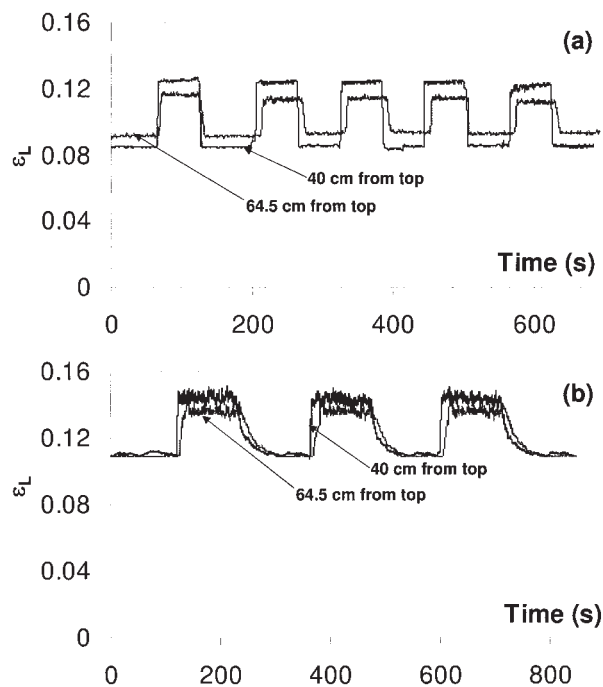


Figure 4. An example of liquid holdup traces during induced pulsing flow, $T_r = 75^\circ\text{C}$, $P_r = 0.7\text{ MPa}$, $u_G = 0.2\text{ m/s}$.

(a) Air-water system, $u_{LB} = 0.0035\text{ m/s}$, $u_{LP} = 0.007\text{ m/s}$, $t_b = 60\text{ s}$, $t_p = 60\text{ s}$; (b) air-0.25%CMC system, $u_{LB} = 0.00087\text{ m/s}$, $u_{LP} = 0.0035\text{ m/s}$, $t_b = 120\text{ s}$, $t_p = 120\text{ s}$.

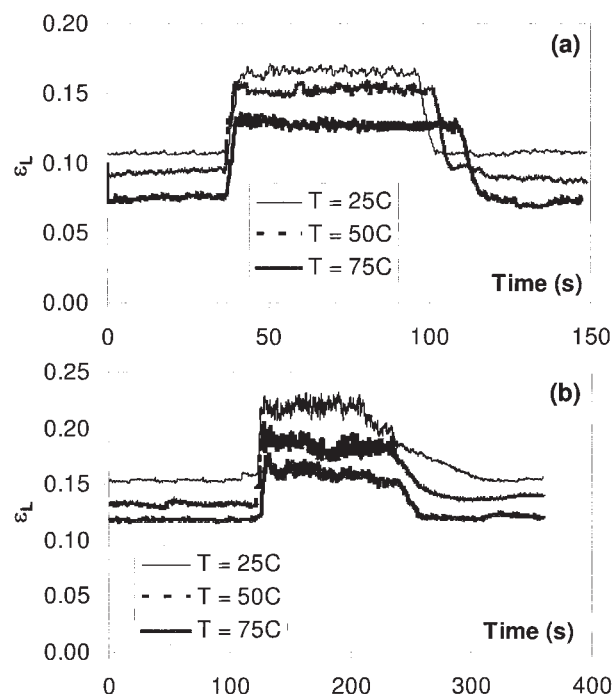


Figure 5. Effect of temperature on shock wave patterns measured 40 cm from bed top, $P_r = 0.3\text{ MPa}$, $u_G = 0.2\text{ m/s}$.

(a) Air-water system, $u_{LB} = 0.0035\text{ m/s}$, $u_{LP} = 0.0105\text{ m/s}$; (b) air-0.25%CMC system, $u_{LB} = 0.00087\text{ m/s}$, $u_{LP} = 0.0035\text{ m/s}$.

clearly highlighted by the variations in B_α shown in Figures 6a and b and measured at 40cm bed depth, independently of the viscous character of the liquid phase, for various pressures, and base and pulse velocity combinations. It is very likely that the shock waves would prematurely vanish after crossing shorter depths in trickle beds operated at higher temperatures. The fact that less sensational contrasts prevail between base and pulse holdups, that is, diminishing B_α values, at increasing temperatures could in all appearance seriously question the opportunity for implementing induced pulsing strategies in high-temperature and especially tall beds. We will see later on that pulse depletion via mass exchange with baseline flow explains only part of the amplitude reduction, whereas another part is ascribed to the reduction of the levels of the base and pulse holdups themselves as temperature rises, which occurs regardless of whether induced pulsing or non-forced continuous TBR flow are in play.

Figures 5a and b show that all four shock wave characteristics, previously depicted in Figure 2a, are altered by an increase in temperature. These morphological features will be discussed in more detail in the forthcoming sections. Note that an overshoot in liquid holdup occurs for the air-0.25% CMC system at the burst of the shock wave. It is unclear, though, to which phenomenon this is to be ascribed since elastic effects were not observed during the rheological characterization of the liquid at such a minute CMC concentration.

The decrease of liquid holdup with temperature appears to be more prominent in the pulse flow regime when higher superficial liquid velocities are used, as exemplified in the case of

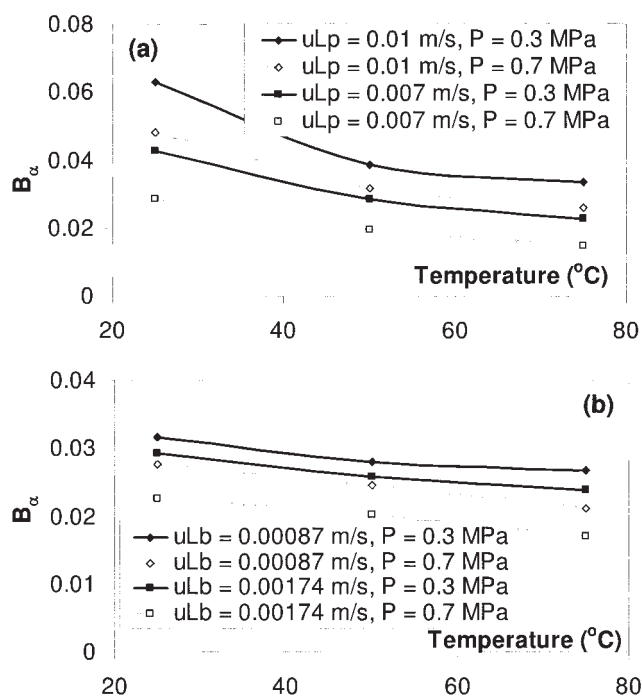


Figure 6. Effect of temperature and pressure on breakthrough amplitude B_α at various base and pulse superficial liquid velocities, $u_G = 0.2$ m/s, measured 40 cm from bed top.

(a) Air-water system, $u_{Lb} = 0.0035$ m/s; (b) air-0.25% CMC system, $u_{Lp} = 0.0035$ m/s.

air-0.25% CMC at $u_{Lp} = 3.5$ mm/s where ε_L as large as about 0.22 can occur (see Figure 5b). Furthermore, the decrease with temperature of pulse holdup is more palpable than for base holdup. This causes the shock wave to decay more quickly the higher the temperature, as clearly suggested from the viscous liquid (Figure 5b) or as depicted by the temperature-dependent variations in breakthrough amplitude, B_α , of Figures 6a and b.

Shock wave patterns versus pressure

Figures 7a and b illustrate the effect of pressure on the shock waves, respectively, for the air-water and air-0.25% CMC systems at a constant temperature of 75°C. In terms of sensitivity of liquid holdup to pressure, our study confirms the decreasing holdup trend with increasing pressures, on a gas superficial basis, as observed already for the continuous-flow TBR operation in the case of ambient¹⁸⁻²⁰ or of elevated temperatures.¹⁵ Liquid holdup underwent reduction for both the pulse and base portions. However, the reduction was more significant for the pulse portion considering that more gas-liquid interactions occur at higher liquid holdup values. It is interesting to note that the effect of pressure on the shock wave decay time is less substantial than in the case of temperature. However, provided the rest of all the operating parameters are unchanged, it appears that higher pressures tend, at a given bed depth, to smooth out the shock wave and to reduce the breakthrough amplitude (see also Figures 6a and b). Clearly, pulse liquid holdups retract as either temperature or pressure is increased. Hence, as for the negative impact of temperature, shock waves would similarly be afflicted by higher pressures.

Extent of pulse-base holdup exchange with temperature and pressure

The previous observations tended to support the contention of a non-isolated nature of pulses in the slow-mode induced pulsing (see Figure 8), as well as the inclination of pulses to get (vertically) squeezed with increasing temperature and/or pressure. However, such behaviors have been inferred based on comparisons between base, ε_{Lb} , and pulse, ε_{Lp} , holdup homologous series recorded at different temperature and pressure levels under otherwise similar conditions. As alluded to earlier, this comparison may be biased since the liquid holdups, ε_{Lb}^o (at u_{Lb}) and ε_{Lp}^o (at u_{Lp}), for the continuous-flow TBR operation at liquid superficial velocities corresponding to the same base, u_{Lb} , and pulse, u_{Lp} , velocities are themselves also prone to changes with temperature and pressure. Therefore, additional liquid holdup experiments have been carried out under continuous-flow TBR operation to quantify the following *deviation indices* between induced pulsing and non-forced continuous flow:

$$\frac{\Delta \varepsilon_{Lp}}{\varepsilon_{Lp}^o} = \frac{\varepsilon_{Lp}^o - \varepsilon_{Lp}}{\varepsilon_{Lp}^o} \quad (2)$$

$$\frac{\Delta \varepsilon_{Lb}}{\varepsilon_{Lb}^o} = \frac{\varepsilon_{Lb} - \varepsilon_{Lb}^o}{\varepsilon_{Lb}^o} \quad (3)$$

Deviation indices equal to zero would suggest, on the one hand, that pulses are isolated and do not transfer their material

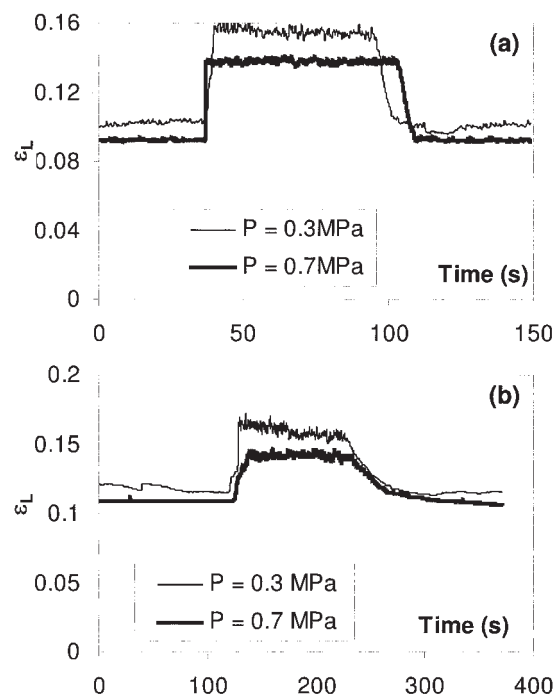


Figure 7. Effect of pressure on shock wave patterns measured 40 cm from bed top, $T_r = 75^\circ\text{C}$, $u_G = 0.2$ m/s.

(a) Air-water system, $u_{Lb} = 0.0035$ m/s, $u_{Lp} = 0.0105$ m/s; (b) air-0.25% CMC system, $u_{Lb} = 0.00087$ m/s, $u_{Lp} = 0.0035$ m/s.

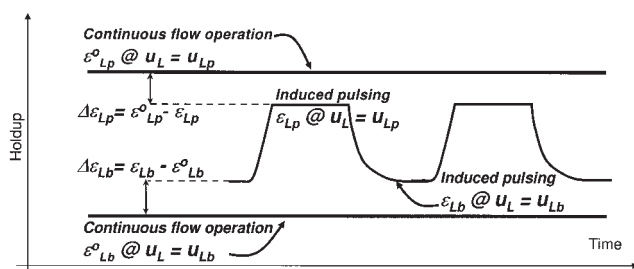


Figure 8. Definition of the deviation indices and distinction between the holdup patterns of induced pulsing and non-forced continuous operation for a given (u_{Lb}, u_{Lp}) set.

content to the baseline flow (that is, subject to u_{Lb} irrigation); and on the other hand, that induced pulsing under such circumstances would reduce to mere juxtaposition of two non-interacting sequences of continuous-flow hydrodynamic states, one at u_{Lb} and the other at u_{Lp} , that would be completely described off induced-pulsing runs. Positive deviation indices would signify that: i) the pulse liquid holdup in liquid induced pulsing suffers a loss with respect to continuous flow at the same u_{Lp} (Figure 8), and ii) the base liquid holdup in liquid induced pulsing undergoes a gain with respect to continuous flow at the same u_{Lb} (Figure 8).

Figures 9a and b show that no other possibility on the signs of the deviation indices exist for our tested conditions. Also, the figures reveal beyond doubt that regardless of the pressure and temperature levels explored here, the pulses in the induced pulsing are indeed non-isolated entities. Since both ε_{Lb}^o and ε_{Lp}^o slip down to lower values with increased temperature and pressure, Figures 9a and b suggest that, in relative proportions, pulses at 0.3 MPa give up about 15% of ε_{Lp}^o at 20°C, reducing to about 3.5% of ε_{Lp}^o at 75°C. Similarly, this exchange would diminish the higher the pressure because of the correspondingly lesser liquid holdup. The base holdup exhibits a similar

behavior as suggested by the evolution of the deviation index given by Eq. 3. However, less viscous liquids witness higher exchange levels between pulse and base than more viscous ones.

Shock wave breakthrough time

The influence of temperature and/or pressure on the shock wave breakthrough time, B_τ , was also studied for both systems, as shown in Figures 10a and b. The shock wave breakthrough time decreases with increasing temperature for the air-water system. A feature presumably ascribable to the water viscosity reduction with temperature enabling, within about 3–4 s, a liquid holdup taking up once liquid feed rate is tipped up. At a given temperature, increased pressure (or gas density) yields stronger gas-liquid interactions and higher gas inertia thus jostling more vigorously the liquid flow and contributing to shorten down to about 2 s the B_α values (Figure 10a). The shock wave breakthrough time also decreases with increasingly base superficial liquid velocity when the same pulse velocity is maintained since, obviously, the gap between pulse and base holdup levels becomes slimmer. For the air-0.25% CMC system, similar effects of temperature, pressure, and base velocities were observed (Figure 10b), with nonetheless more pronounced temperature effect plausibly attributable to more drastic viscosity drops.

Shock wave plateau time

One additional parameter characterizing pulse morphology is the shock wave plateau time, P_τ . At constant base superficial liquid velocity, the effects of pulse superficial liquid velocity, reactor temperature, and pressure on P_τ for the air-water and air-0.25% CMC systems are illustrated in Figures 11a and b. Recall that the feed policy delivers perfectly rectangular inlet pulses with plateau times lasting 60 s for water and 120 s for aqueous 0.25% CMC solution. At constant temperature and pressure, the shock wave plateau time increases with pulse

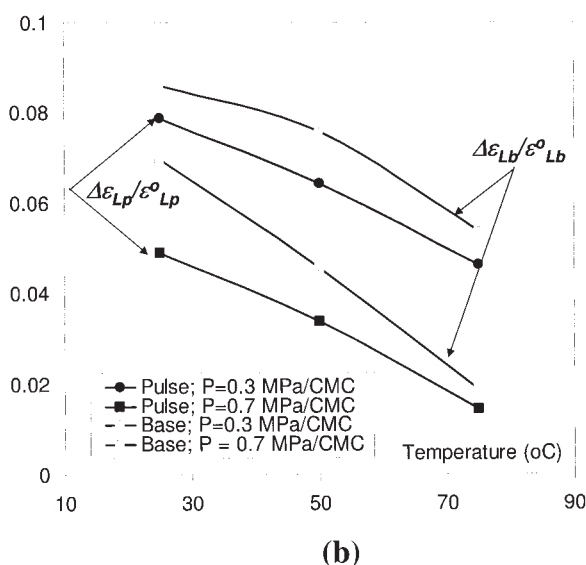
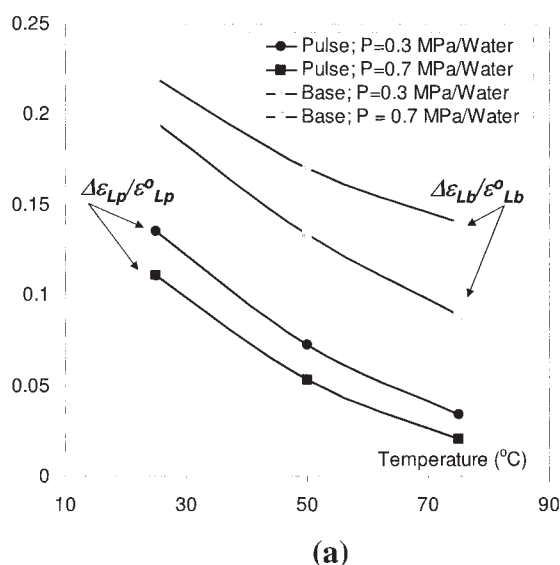


Figure 9. Deviation indices (Eqs. 2 and 3) as a function of temperature and pressure obtained at 40cm depth.

$u_G = 0.2$ m/s. (a) air-water system, $u_{Lp} = 0.014$ m/s; (b) air-0.25% CMC system, $u_{Lp} = 0.0035$ m/s.

superficial liquid velocity. In the same manner, the shock wave plateau time increases with increasing temperature and/or pressure for the air-water system, though the effect of temperature is more pronounced. At first glance, plateaus lasting less than 60 s would simply be interpreted as being amputated of their breakthrough time and decay time (to be discussed in the next section), especially at the lower pulse superficial velocity values (Figure 11a). However, $P_r > 60$ s were measured, particularly when larger pulse velocities coincide with elevated temperatures and pressures (right region of Figure 11a). Hence, an additional feature of the pulse morphology stems here that indicates that pulses collapse not only because they transfer some of their cargo to the baseline flow as noted previously but also because pulses flatten, presumably owing to dispersive effects that result in stretching the plateau times. The air-0.25% CMC system, at constant pulse superficial liquid velocity, exhibits shock wave plateau increasing with increasing pressure similar to the air-water system, but this effect is less substantial at high pulse superficial velocity. Note that for this system, P_r is always less than 120 s because of the dominant effect of the breakthrough time and especially the decay time, as shown in Figures 4b, 5b, and 7b.

Shock wave decay time

Figures 12a and b depict the evolution of the decay time, D_r , of the shock wave versus the base superficial liquid velocity for the air-water and the air-0.25% CMC systems plotted at different temperatures and pressures. In a fashion similar to the previous observation regarding the breakthrough time, the de-

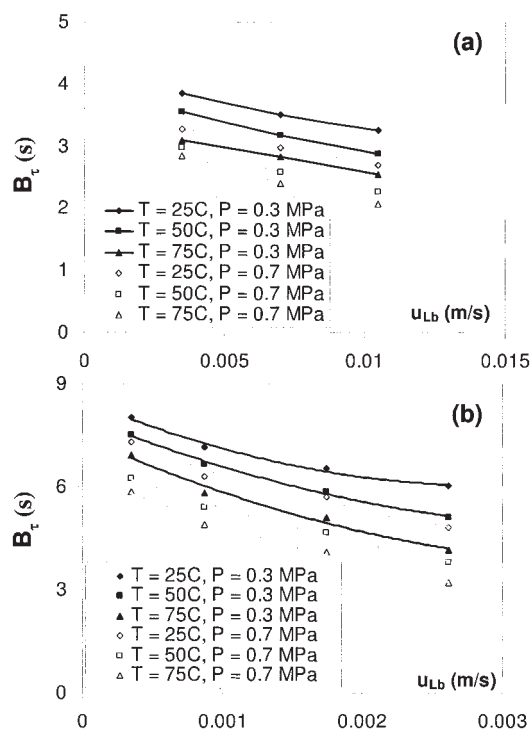


Figure 10. Shock wave breakthrough time as a function of base superficial liquid velocity.

Effect of reactor temperature and pressure. $u_G = 0.2 \text{ m/s}$. (a) air-water system, $u_{Lp} = 0.0175 \text{ m/s}$; (b) air-0.25% CMC system, $u_{Lp} = 0.0035 \text{ m/s}$.

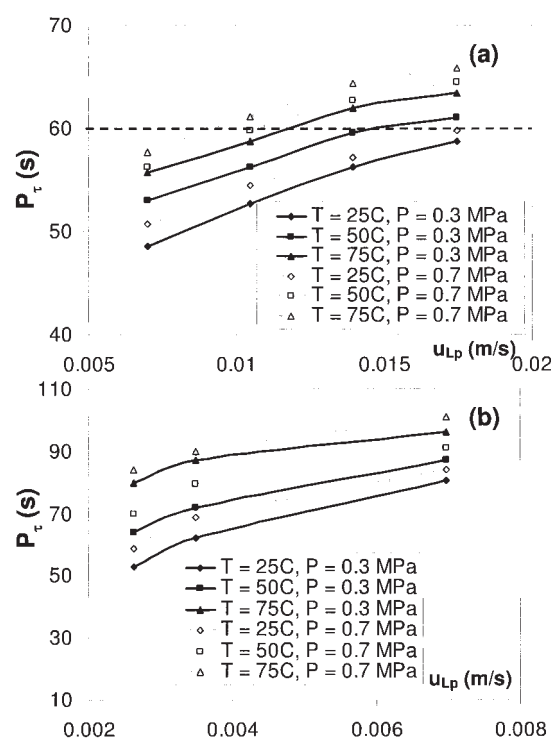


Figure 11. Influence of pulse superficial liquid velocity, temperature, and pressure on plateau time, $u_G = 0.2 \text{ m/s}$.

(a) Air-water system, $u_{Lb} = 0.0035 \text{ m/s}$; (b) air-0.25% CMC system, $u_{Lb} = 0.00087 \text{ m/s}$.

cay time tendency to thinning is favored by increased base superficial liquid velocity at constant temperature, pressure, and pulse velocity. This observation is in agreement with observations made by previous researchers for ambient temperature and atmospheric pressure tests.¹ At constant base superficial liquid velocity, the shock wave decay time decreases with the temperature and pressure and can be easily explained taking again the same interpretive arguments as for the breakthrough time behavior (Figure 10).

For the air-water system, temperature and pressure appeared to be more influential the lower the base superficial liquid velocity. Furthermore, as the pulse holdup decreases more notably than the base holdup with increased temperature and/or pressure (Figure 5a), the corresponding decrease in breakthrough amplitude, B_α , results into less substantial effects from temperature and pressure, especially at higher base superficial liquid velocities, explaining thus the retracting decay times (Figure 12a). For the air-0.25% CMC system, the shock wave decay time also decreases with increasing base superficial liquid velocity, temperature, and pressure. Contrary to the air-water system, the effect of temperature and pressure on the shock wave decay time is more pronounced the higher the base superficial liquid velocities. Additionally, the effect of pressure on the shock wave decay time for the non-Newtonian liquid is less significant than for the Newtonian liquid. Though D_r is characterized by the formation of a long tail,¹ this latter will be less prominent the higher the temperature or pressure.

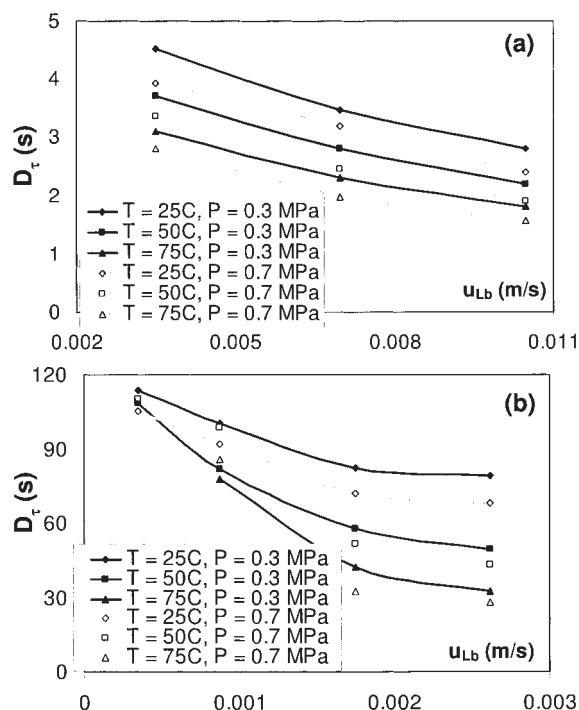


Figure 12. Influence of base superficial liquid velocity, temperature, and pressure on decay time, $u_{G} = 0.2$ m/s.

(a) Air-water system, $u_{Lp} = 0.0175$ m/s; (b) air-0.25% CMC system, $u_{Lp} = 0.0035$ m/s.

Shock wave breakthrough amplitude

Going back to Figures 6a and b, these latter illustrate the effect of pressure and temperature on the breakthrough amplitude, B_{α} . For the air-water system, B_{α} decreases with increased temperature with a marked effect of the latter, the higher the pulse superficial velocities (Figure 6a). The breakthrough amplitude also decreases with increased pressure, especially at low temperature. Similarly, B_{α} decreases with temperature and pressure for the air-0.25% CMC system, though to a much lesser extent in comparison with the air-water system. At elevated temperature and pressure, the decrease in B_{α} also means diminishing pulse liquid holdup. Recall that the most beneficial purpose put forward for liquid induced pulsing is to remove excessive incipient heat of the reaction and problematical products from the catalyst surface while supplying fresh liquid phase reactants. At industrial conditions where elevated temperature and pressure are often required, it would be difficult to fully benefit from the potential of induced pulsing should the scale up be based on the amplitudes measured in cold flow conditions.

Shock wave velocity

The shock wave velocity, V_s , was determined at elevated pressure and temperature at different superficial gas and pulse liquid velocities for air-water and air-0.25% CMC systems (Figures 13a and b) where the experimental data were compared with the Wallis²¹ shock wave velocity relationship. As seen from Figure 13a, the shock wave velocity increases with temperature and pressure at constant superficial gas, base, and

pulse liquid velocities for the air-water system. The decrease of pulse holdup is more severe compared to the decrease in base holdup with increased temperatures, causing the shock wave velocity to increase. However, our measurements were found to be systematically over-predicted by the Wallis shock wave velocity equation.²¹ This provides a further confirmation of the deviation of TBR induced pulses from the ideal square-wave cycling assumed by the Wallis²¹ relationship. For the air-0.25% CMC system, the shock wave velocity increases with temperature and pressure, everything else being kept constant (Figure 13b). The shock wave velocity values are lower than for the air-water system due to larger viscosity and, thus, larger liquid holdup exhibited by the 0.25% CMC solution. At constant temperature and pressure, the shock wave velocity was found to increase with superficial gas velocity coherent with the corresponding decrease in liquid holdup.

Pulse frequency

The base-level portion of the induced pulsing experiments always took place in the trickle flow regime, whereas the pulse flow regime was allowed to occur in the pulse portion for sufficiently high values of u_{Lp} . Maintaining constant base (low-level) superficial liquid velocity constant, the pulse frequency, f , was measured in various conditions of high-level (pulse) liquid feed rate experiments when the pulse flow regime was

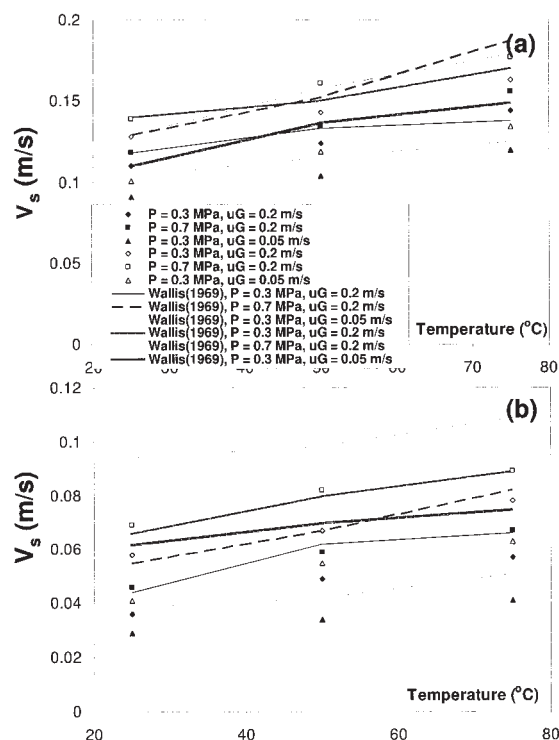


Figure 13. Effect of temperature and pressure on the shock wave velocity.

Experimental vs. calculated values. (a) air-water system, filled symbols represent data for $u_{Lb} = 0.0035$ m/s, $u_{Lp} = 0.014$ m/s; empty symbols represent data for $u_{Lb} = 0.0035$ m/s, $u_{Lp} = 0.0175$ m/s; (b) air-0.25% CMC system, filled symbols represent data for $u_{Lb} = 0.00087$ m/s, $u_{Lp} = 0.0035$ m/s; and empty symbols data for $u_{Lb} = 0.00087$ m/s, $u_{Lp} = 0.007$ m/s.

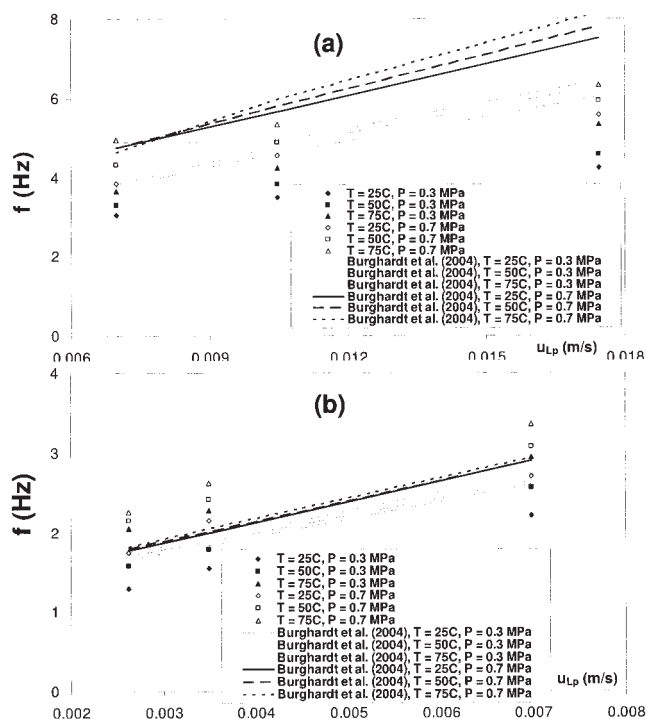


Figure 14. Effect of temperature and pressure on pulse frequency.

Experimental vs. calculated values, $u_G = 0.2$ m/s. (a) air-water system, $u_{Lb} = 0.0035$ m/s; (b) air-0.25% CMC system, $u_{Lb} = 0.00087$ m/s.

attained for both air-water and air-0.25% CMC systems. The experimental values obtained at elevated temperature and pressure are plotted together with the frequency values calculated by the correlation suggested by Burghardt et al.²² for the air-water and air-0.25% CMC systems in Figures 14a and b. Figure 14a shows that the pulse frequency increases with pulse superficial liquid velocity at constant temperature. In the same manner, at constant pulse superficial liquid velocity, pulse frequency increases with increased temperature and pressure for the air-water system. The frequency values predicted with the correlation of Burghardt et al.²² are higher than the experimental values. For the air-0.25% CMC system and at lower pressure, the experimental and calculated pulse frequency values are closer. However, the correlation predicts lower frequency values at elevated pressure.

Conclusion

Operating the column in liquid induced pulsing flow is proposed as one of the strategies for process intensification in TBRs. As industrial TBRs operate at elevated temperature and pressure; the necessity of investigating the effect of temperature and/or pressure on the TBR performance exploiting this strategy is a central topic. Previous investigations focusing on liquid induced pulsing flows were performed at atmospheric pressure and ambient temperature. In this study, the aim was to illustrate the effects of temperature and pressure on the shock wave characteristics for both Newtonian and non-Newtonian liquids. The decay process for the shock waves was found to reduce with increased temperature and pressure. The shock

wave breakthrough time and shock wave decay time decreased with increasing temperature and pressure. On the contrary, the shock wave plateau time increased with temperature and pressure. This would favor the removal of heat and products from the catalyst during the high liquid feed. However, the liquid holdup decreased with temperature, especially at the high liquid feed rates. This phenomenon could be viewed as an obstacle for enhancement of reactor performance with liquid induced pulsing flow at high temperature and pressure operations. The shock wave velocity and the pulse frequency were found to increase with temperature and pressure.

Acknowledgments

Financial support from the Natural Sciences and Engineering Research Council of Canada (NSERC) is gratefully acknowledged. D.F. would also like to extend her gratitude to the Ernest-Solvay-Foundation for a scholarship.

Notation

B_α = breakthrough amplitude, –
 B_x = breakthrough time, s
 D_τ = decay time, s
 f = pulse frequency, Hz
 u = superficial velocity, m/s
 P_r = reactor pressure, MPa
 P_τ = plateau time, s
 t = time, s
 T_r = reactor temperature, °C
 V_s = shock wave velocity, m/s

Greek letters

ε_L = liquid holdup

Subscripts

b = base
 G = gas phase
 L = liquid phase
 o = continuous-flow TBR operation
 p = pulse
 r = reactor

Literature Cited

- Boelhouwer JG, Piepers HW, Drinkenburg AAH. Liquid-induced pulsing flow in trickle-bed reactors. *Chem Eng Sci.* 2002;57:3387-3399.
- Boelhouwer JG, Piepers HW, Drinkenburg AAH. Nature and characteristics of pulsing flow in trickle-bed reactors. *Chem Eng Sci.* 2002; 57:4865-4876.
- Boelhouwer JG, Piepers HW, Drinkenburg AAH. Advantages of forced non-steady operated trickle-bed reactors. *Chem Eng Tech.* 2002;25:647-650.
- Dudukovic MP, Larachi F, Mills PL. Multiphase catalytic reactors: a perspective on current knowledge and future trends. *Catal Rev-Sci Eng.* 2002;44:123-246.
- Nigam KDP, Larachi F. Process intensification in trickle-bed reactors. *Chem Eng Sci.* 2005;60:5880-5894.
- Wilhite BA, Wu R, Huang X, McCready MJ, Varma A. Enhancing performance of three-phase catalytic packed-bed reactors. *AIChE J.* 2001;47:2548-2556.
- Wu R, McCready MJ, Varma A. Effect of pulsing on reaction outcome in a gas-liquid catalytic packed-bed reactor. *Catal Today.* 1999;48: 195-198.
- Haure PM, Hudgins RR, Silveston PL. Periodic operation of a trickle-bed reactor. *AIChE J.* 1989;35:1437-1444.
- Lange R, Hanika J, Stradiotto D, Hudgins RR, Silveston PL. Investi-

- gations of periodically operated trickle-bed reactors. *Chem Eng Sci.* 1994;49:5615-5621.
10. Tukac V, Hanika J, Chyba V. Periodic state of wet oxidation in trickle-bed reactor. *Catal Today.* 2003; 79-80: 427-431.
 11. Wilhite BA, Huang X, McCready MJ, Varma A. Effects of induced pulsing flow in trickle-bed reactor performance. *Indus Eng Chem Res.* 2003;42:2139-2145.
 12. Urseanu MI, Boelhouwer JG, Bosman HJM, Schroyen JC. Induced pulse operation of high-pressure trickle bed reactors with organic liquids: hydrodynamics and reaction study. *Chem Eng Proc.* 2004;43: 1411-1416.
 13. Xiao Q, Cheng ZM, Jiang ZX, Anter AM, Yuan WK. Hydrodynamic behavior of a trickle bed reactor under "forced" pulsing flow. *Chem Eng Sci.* 2001;56:1189-1195.
 14. Giakoumakis D, Kostoglou M, Karabelas AJ. Induced pulsing in trickle beds—characteristics and attenuation of pulses. *Chem Eng Sci.* 2005;60:5183-5197.
 15. Aydin B, Larachi F. Trickle bed hydrodynamics and flow regime transition at elevated temperature for a Newtonian and a non-Newtonian liquid. *Chem Eng Sci.* 2005;60:6687-6701.
 16. Iliuta I, Larachi F. Hydrodynamics of power-law fluids in trickle-flow reactors: mechanistic model, experimental verification and simulations. *Chem Eng Sci.* 2002;57:1931-1942.
 17. Tsochatzidis NA, Karabelas AJ. Properties of pulsing flow in a trickle bed. *AIChE J.* 1995;41:2371-2382.
 18. Wammes WJA, Westerterp KR. The influence of the reactor pressure on the hydrodynamics in a cocurrent gas-liquid trickle bed reactor. *Chem Eng Sci.* 1990;45:2247-2254.
 19. Larachi F, Laurent A, Midoux N, Wild G. Experimental study of a trickle bed reactor operating at high pressure: two-phase pressure drop and liquid saturation. *Chem Eng Sci.* 1991;46:1233-1246.
 20. Al-Dahhan MH, Dudukovic MP. Pressure drop and liquid holdup in high pressure trickle bed reactors. *Chem Eng Sci.* 1994;49:5681-5698.
 21. Wallis GB. *One-Dimensional Two-Phase Flow*. New York: McGraw-Hill, Inc.; 1969.
 22. Burghardt A, Bartelmus G, Szlemp A. Hydrodynamics of pulsing flow in three-phase fixed-bed reactor operating at an elevated pressure. *Indus Eng Chem Res.* 2004;43:4511-4521.

Manuscript received May 8, 2006, and revision received Aug. 2, 2006.